20

Neutrino masses and mixing: experimental results

The cross-sections for neutrino–lepton and neutrino–quark interactions are exceedingly small: the collection of data from a particular experiment may extend over several years. The aims of neutrino experiments include: establishing the existence of neutrino oscillations, checking the validity of the theory of Chapter 19, measuring the parameters of the mixing matrix **U** and determining the mass eigenstates of the neutrino. In this chapter we shall present some results of recent experimental work, and indicate how they have been obtained.

20.1 Introduction

Setting aside the possible existence of sterile neutrinos, it is thought that there are three neutrino mass eigenstates, which we shall label by $i = 1, 2, 3$. Measurements of neutrino oscillations give (mass)^2 differences:

$$\Delta m_{ij}^2 = m_i^2 - m_j^2.$$

It is estimated from experiment that

$$1.3 \times 10^{-3}\ \text{eV}^2 < |\Delta m_{32}^2| < 3 \times 10^{-3}\ \text{eV}^2,$$

and

$$6.5 \times 10^{-5}\ \text{eV}^2 < |\Delta m_{21}^2| < 8.5 \times 10^{-5}\ \text{eV}^2.$$

Then $\Delta m_{31}^2 = \Delta m_{32}^2 + \Delta m_{21}^2$.

For illustrative numerical calculations in this chapter we shall take $|\Delta m_{32}^2| = 2 \times 10^{-3}\ \text{eV}^2$ and $|\Delta m_{21}^2| = 7 \times 10^{-5}\ \text{eV}^2$.

https://doi.org/10.1017/9781009401685.022 Published online by Cambridge University Press

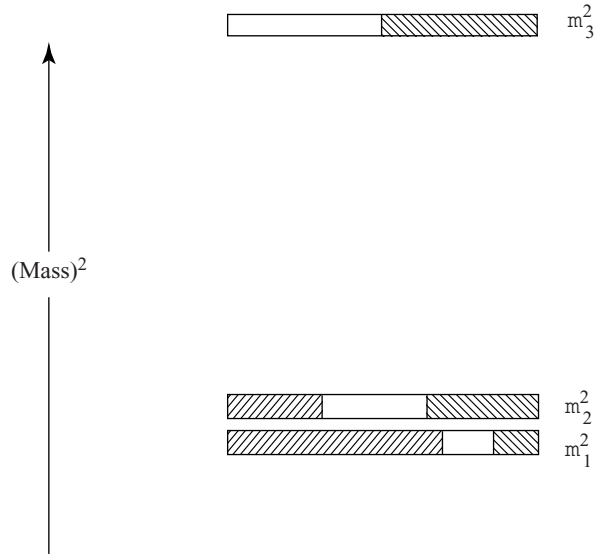

Figure 20.1 A three neutrino mass-squared spectrum. The ν_e fraction of each mass eigenstate is indicated by right-leaning hatching, the ν_μ fraction is blank and the ν_τ fraction by left-leaning hatching (see the report by B. Kayser, Particle Data Group, 2004). The mass-squared base line is not known.

The 3×3 unitary mixing matrix is approximately

$$\mathbf{U} = \begin{bmatrix} c & s & s_{e3}e^{i\delta} \\ -s/\sqrt{2} & c/\sqrt{2} & 1/\sqrt{2} \\ s/\sqrt{2} & -c/\sqrt{2} & 1/\sqrt{2} \end{bmatrix} \tag{20.1}$$

where $c \approx \cos\theta_{e2} \approx 0.84$ and $s \approx \sin\theta_{e2} \approx 0.54$.

It is estimated that $|s_{e3}|^2 < 0.05$. A term $s_{e3}e^{i\delta}$ with $\sin\delta \neq 0$ would violate *CP* conservation and lead to matter–antimatter asymmetry. Such asymmetry has not yet (2006) been discerned. If $s_{e3} \neq 0$ there are small complex corrections to other elements of the matrix. (The matrix (20.1) may be obtained from the unitary KM matrix of Section 14.3 by taking $c_{13}(=c_{e3}) = 1$, $c_{12}\,(=c_{e2}) = c$, $c_{23}(=c_{\mu 3}) = 1/\sqrt{2}$, $s_{13} = s_{e3}$).

The $(\text{mass})^2$ differences imply either a spectrum of $(\text{mass})^2$ eigenstates as in Fig. 20.1, with the closest eigenstates having the smallest mass, or the figure might be inverted, with the closest $(\text{mass})^2$ eigenstates the heaviest. The mixing matrix determines the fractions of ν_e, ν_μ and ν_τ states making up the states 1, 2, 3, and these are indicated on the figure.

In many data analyses the approximation is made of setting $s_{e3} = 0$. We shall see that any particular analysis is then greatly simplified since the number of participating neutrino mass eigenstates is reduced from three to two. Apart from our

https://doi.org/10.1017/9781009401685.022 Published online by Cambridge University Press

discussion of the CHOOZ experiment, we shall always make this approximation. However, as the quality of data improves, and in particular when and if s_{e3} is seen to be finite, the approximation will be abandoned. It is important to note that with $s_{e3} = 0$ there is no *CP* violation.

The analysis of data from accelerator and reactor neutrinos is the least complicated, since the MSW effect is negligible at the levels of precision so far obtained, and our formula (19.19) can be directly invoked.

20.2 K2K

The Japanese K2K experiment studies a muon neutrino beam that is engineered at the KEK proton accelerator. 12 GeV protons hit an aluminium target, producing mainly positive pions that decay $\pi^+ \to \mu^+ + \nu_\mu$ (Section 9.2). The beam characteristics are measured by near detectors located 300 m down-stream from the proton target. The mean ν_μ energy is 1.3 GeV. There is then a 250 km flight path to the Super-Kamiokandi detector in the Komioka mine. This detector consists of 22.5 kilotonnes of very pure water (H_2O). Muon neutrinos are observed through their reaction with neutrons in the oxygen nuclei: $\nu_\mu + n \to p + \mu^-$. The neutrino energy E_ν can be determined from measurements of the energy and direction of the muon.

To reach the detector, a neutrino has to pass through the Earth's upper crust. However, we ignore any MSW effect for the moment, and take the values of Δm^2_{21} given in Section 20.1. $\Delta m^2_{21} = 7 \times 10^{-5}\,\text{eV}^2$ and $D = 250\,\text{km}$. From (19.20) the oscillating function $\sin^2\left(\dfrac{\Delta m^2_{21} D}{4E_\nu}\right) = \sin^2\left(0.022\left(\dfrac{1\,\text{GeV}}{E_\nu}\right)\right) < 10^{-3}$ for all relevant E_ν. This is so small that with present precision it can be ignored. Also, since $\Delta m^2_{31} = \Delta m^2_{32} + \Delta m^2_{21}$ the two other oscillating functions are almost equal, and we will take them both as $\sin^2\left(\dfrac{\Delta m^2_{At} D}{4E_\nu}\right)$ with Δm^2_{At} a mean value of Δm^2_{32} and Δm^2_{31}. For historical reasons Δm^2_{At} is called the *atmospheric mass squared difference.*

With these approximations, setting $U_{e3} = 0$ and using the unitarity of U, equations (19.19) give

$$\begin{aligned} P_D(\nu_\mu \to \nu_\mu) &= 1 - 4|U_{\mu 3}|^2(1 - |U_{\mu 3}|^2)\sin^2\left(\frac{\Delta m^2_{\text{At}} D}{4E_\nu}\right), \\ P_D(\nu_\mu \to \nu_e) &= 0, \\ P_D(\nu_\mu \to \nu_\tau) &= 4|U_{\mu 3}|^2(1 - |U_{\mu 3}|^2)\sin^2\left(\frac{\Delta m^2_{\text{At}} D}{4E_\nu}\right). \end{aligned} \tag{20.2}$$

From these equations, and because of the smallness of $|U_{e3}|^2$, the ∇m^2_{At} oscillation is almost entirely between ν_μ and ν_τ. Since the MSW effect is for electron

https://doi.org/10.1017/9781009401685.022 Published online by Cambridge University Press

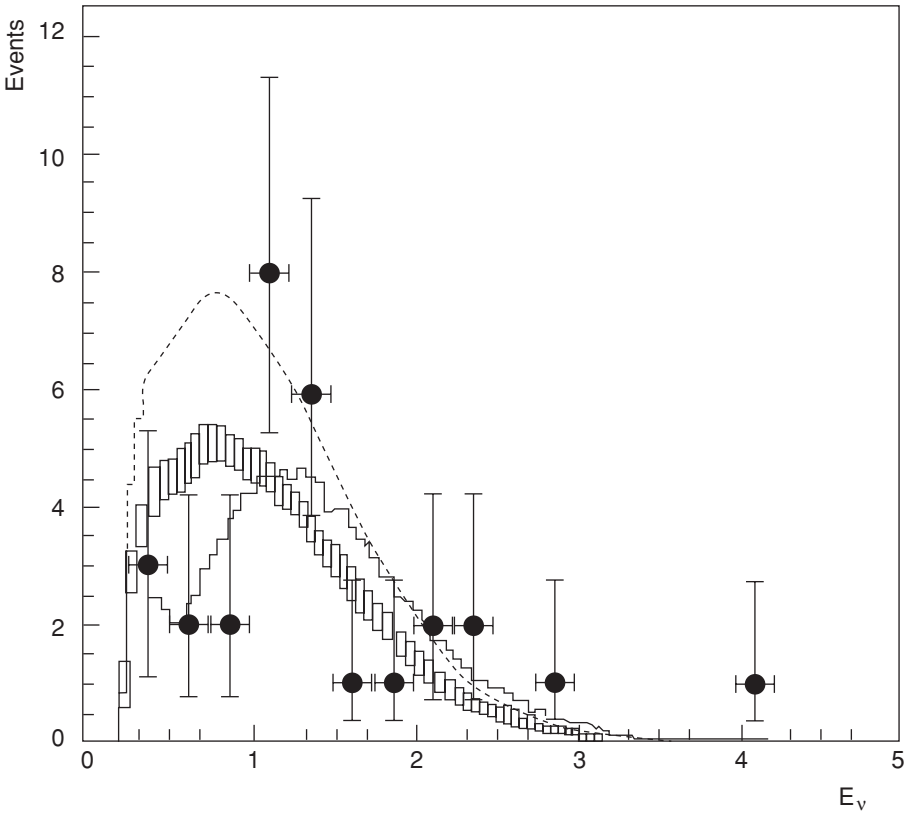

Figure 20.2 K2K data (M. H. Ahn *et al*. *Phys. Rev. Letts*. **90**, 041801 (2003)). Points with error bars are data. The box histogram is the expected spectrum without oscillations, where the height of the box is the systematic error. The solid line is the best-fit spectrum. These histograms are normalised by the number of events observed (29). In addition, the dashed line shows the expectation with no oscillations normalised to the expected number of events (44).

neutrinos only, it can with present precision be neglected. With $U_{e3} = 0$, we have $|U_{\mu 3}| = \sin\theta_{\mu 3}$ and we arrive at our final formula:

$$P_D(\nu_\mu \to \nu_\mu) = 1 - \sin^2(2\theta_{\mu 3}) \sin^2\left(\frac{\Delta m^2_{\rm At} D}{4E_\nu}\right) \tag{20.3}$$

for fitting the K2K data. This is presented in Fig. 20.2 in which the number of events in the designated energy bins are shown as a function of the mean neutrino energy of each bin. The dashed curve is the expected number distribution $\mathrm{d}N/\mathrm{d}E_\nu$ without oscillation, and when integrated over E_ν is clearly larger than the total number (29) of events accepted. The best fit with equation (20.3), modified to take account of corrections such as energy resolution, is also shown.

https://doi.org/10.1017/9781009401685.022 Published online by Cambridge University Press

It corresponds to $\Delta m^2_{\rm At} = 2.8 \times 10^{-3}\,{\rm eV}^2$ and $\sin^2(2\theta_{\mu 3}) = 1$. The latter allows $\theta_{\mu 3} = \pi/4,\ \cos\theta_{\mu 3} = \sin\theta_{\mu 3} = 1/\sqrt{2}$.

20.3 Chooz

Chooz is a village close to a French nuclear power station. The power station's two reactors are rich sources of electron antineutronos $\bar{\nu}_{\rm e}$. The fluxes and energy distributions, centred around 3 MeV, of these antineutrinos are very well understood. The detector, shielded from cosmic ray muons by its location deep underground, was positioned about 1 km from the reactors.

The antineutrinos $\bar{\nu}_{\rm e}$ were detected by their inverse β decay interaction with protons, $\bar{\nu}_{\rm e} + {\rm p} + 1.8\,{\rm MeV} \rightarrow {\rm n} + {\rm e}^+$, in a hydrogen rich paraffinic liquid scintillator.

As with the K2K experiment, the oscillatory function $\sin^2\left(\Delta m^2_{21} D/4E_\nu\right)$ is, from (19.20), negligibly small, $< 2 \times 10^{-3}$ (taking $D = 1$ km, $E_\nu > 1.8$ MeV). The MSW effect can also be neglected, since for material in the Earth's crust $V(z) \sim 10^{-13}\,{\rm eV} \ll \Delta m^2_{21}/2E_\nu < \Delta m^2_{32}/2E_\nu$. We can, again, to a good approximation, put $\Delta m^2_{32} D/4E_\nu = \Delta m^2_{31} D/4E_\nu = \Delta m^2_{\rm At} D/4E_\nu$ to obtain

$$P_D(\bar{\nu}_{\rm e} \rightarrow \bar{\nu}_{\rm e}) = 1 - 4|U_{\rm e3}|^2\left(1 - |U_{\rm e3}|^2\right)\sin^2\left(\Delta m^2_{\rm At} D/4E_\nu\right). \tag{20.4}$$

Setting $|U_{\rm e3}| = \sin\theta_{\rm e3},\ D = 1\,{\rm km},\ \Delta m^2_{\rm At} = 2 \times 10^{-3}\,{\rm eV}^2$, we find from (19.20)

$$P_D(\bar{\nu}_{\rm e} \rightarrow \bar{\nu}_{\rm e}) = 1 - \sin^2(2\theta_{\rm e3})\sin^2[2.54(3\,{\rm MeV}/E_\nu)].$$

To the experimental precision obtained, there was no reduction in flux at the detector and no oscillation, and it was concluded (Apollonio *et al.*, 2003) that $\sin^2(2\theta_{\rm e3}) < 0.18$, which implies $|U_{\rm e3}|^2 =< 0.05$, the result we quote in Section 20.1 of this chapter.

20.4 KamLAND

Like Chooz, the Kamioka Liquid scintillator AntiNeutrino Detector (KamLAND) experiment uses reactor antineutrinos. The sources are a group of nuclear power stations in Japan situated at various distances $\sim$ 100 km to 200 km from the detector. As at Chooz, the detector makes use of the inverse β decay $\bar{\nu}_{\rm e} + {\rm p} \rightarrow {\rm n} + {\rm e}^+$.

The experiment was designed to explore the $\Delta m^2_{21} \sim 7 \times 10^{-5}\,{\rm eV}^2$ mass region. For a particular reactor at distance D from the detector, we have from (19.19) and setting $|U_{\rm e3}|^2 = 0$, that the survival probability is given by

$$P_D(\bar{\nu}_{\rm e} \rightarrow \bar{\nu}_{\rm e}) = 1 - 4|U_{\rm e1}|^2|U_{\rm e2}|^2\sin^2\left(\frac{\Delta m^2_{21} D}{4E}\right) \tag{20.5}$$

https://doi.org/10.1017/9781009401685.022 Published online by Cambridge University Press

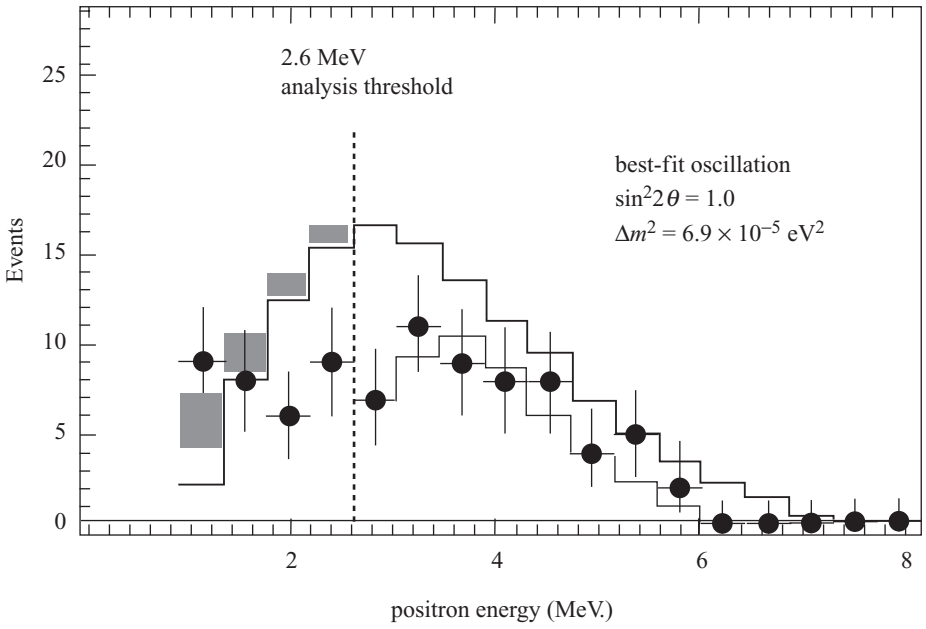

Figure 20.3 KamLAND data (K. Eguchi *et al*. *Phys. Rev. Lett* **90**, 021802 (2003)). The energy distribution of the observed positrons in bins of 0.425 MeV (solid circles with error bars), along with the expected no oscillations distribution (upper histogram) and the best fit including oscillations using (20.5) (lower histogram). The shaded bands indicate the systematic error in the best fit distribution. The vertical dashed line corresponds to the analysis threshold at 2.6 MeV.

and from the parameterization (14.16)

$$4|U_{e1}|^2|U_{e2}|^2 = \cos^4\theta_{e3}\sin^2 2\theta_{e2} \approx \sin^2 2\theta_{e2}.$$

As at Chooz, MSW effects are negligible. The measured positron energy spectrum is compared with the positron energy spectrum that would be expected if there were no antineutrino oscillations. This spectrum can be very well estimated from knowledge of the various reactor characteristics.

Some results from KamLAND are shown in Fig. 20.3. The energy spectrum of the positrons is clearly below what it would be without oscillation. The best fit to the data using an expression based on (20.5) has

$$|m^2_{21}| = 6.9 \times 10^{-5}\,\text{eV}^2,$$
$$0.84 < \sin^2 2\theta_{e2} < 1.$$

The KamLAND analysis took some account of systematic errors arising from the simplifying assumption $|U_{e3}|^2 = 0$.

https://doi.org/10.1017/9781009401685.022 Published online by Cambridge University Press

20.5 Atmospheric neutrinos

The Earth is continually bombarded by cosmic rays, which consist for the most part of high energy protons and electrons. The protons, in their collisions with nuclei in the upper atmosphere, produce π mesons. The π mesons decay by the chains (Section 9.2, Section 9.4):

$$\pi^+ \to \mu^+ + \nu_\mu \quad , \quad \pi^- \to \mu^- + \bar{\nu}_\mu$$
$$\hookrightarrow e^+ + \nu_e + \bar{\nu}_\mu \qquad\qquad \hookrightarrow e^- + \bar{\nu}_e + \nu_\mu \quad .$$

The neutrinos and antineutrinos are produced at a mean height $\sim 20\,\text{km}$, with energies extending to the multi-GeV region. The ratio of the flux $\nu_\mu + \bar{\nu}_\mu$ to the flux of $\nu_e + \bar{\nu}_e$ is evidently about 2.

In water detectors, such as Super Kamiokandi, charged leptons are produced through reactions essentially of the form

$$\nu_e + n \to e^- + p, \qquad \bar{\nu}_e + p \to e^+ + n\,;$$
$$\nu_\mu + n \to \mu^- + p, \qquad \bar{\nu}_\mu + p \to \mu^+ + n.$$

The charged leptons emit Cerenkov radiation, which provides information on the energy, direction and identity of the incident neutrino.

Figure 20.4 shows some results from the Super-Kamiokandi detector. The plots show the ratio of observed ν_e- and ν_μ-like events to Monte Carlo calculations in the absence of oscillations, as a function of D/E_ν. E_ν is the neutrino energy and D the distance from the point of production ~ 20 km above the Earth's surface, to the detector. D is then inferred from the measured neutrino direction. For multi-GeV electron neutrinos, the MSW modification to the equations has to be included for those neutrinos passing through the Earth on their way to the detector.

The ν_e data show no sign of oscillation, but there is a clear deficit of muon neutrinos. The best fit to the data has $\Delta m^2_{\text{At}} = 2.2 \times 10^{-3}\ \text{eV}^2$, and like K2K has $\sin^2 2\theta_{\mu 3} = 1$, where for $D/E_\nu < 10^3\,\text{km/GeV}$ the Δm^2_{32} and Δm^2_{31} oscillations are combined into one Δm^2_{At} oscillation. The absence of discernible $\nu_e \to \nu_e$ oscillations in the data was the first indication of the smallness of $|U_{e3}|^2$, which again implies that the Δm^2_{At} oscillations are predominantly between ν_μ and ν_τ.

20.6 Solar neutrinos

The nuclear and thermal physics of the Sun is well understood. The solar neutrino spectra predicted by the Standard Solar Model and shown in Fig. 20.5 may be assumed with confidence.

https://doi.org/10.1017/9781009401685.022 Published online by Cambridge University Press

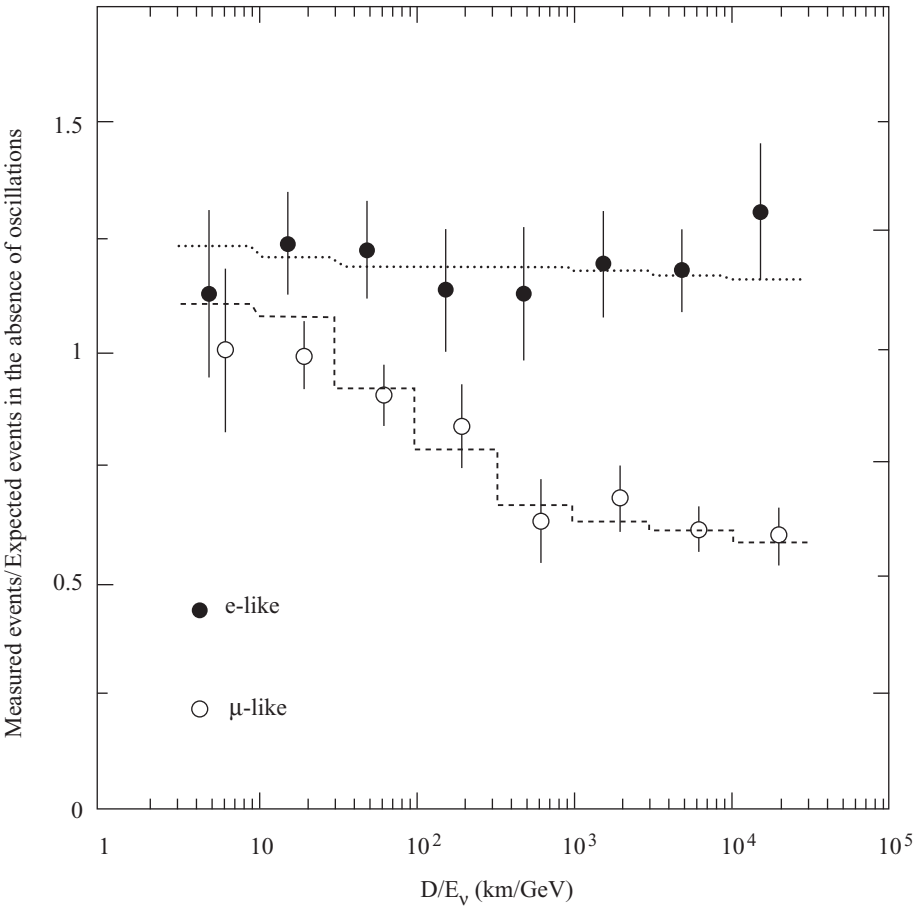

Figure 20.4 Data from Super Kamiokande (Y. Fukunda *et al*. *Phys*. *Rev. Lett.* **82**, 1562 (1998). The ratio of measured events to expected events in the absence of oscillations. The lines show the expected shape for $\nu_\mu \leftrightarrow \nu_\tau$ with $\Delta m^2_{\mathrm{At}} = 2.2 \times 10^{-3}\,\mathrm{eV}^2$ and $\sin^2(2\theta_{\mu 3}) = 1$. There is no significant $\nu_e \leftrightarrow \nu_e$ oscillation observed.

The first measurements of the spectra were made by R. Davis and his collaborators in the deep Homestake mine in the U.S.A, (Davis 1964). The detection of the neutrinos was made through the reaction

$$\nu_e + {}^{37}_{17}\mathrm{Cl} + 0.81\ \mathrm{MeV} \rightarrow e^- + {}^{37}_{18}\mathrm{Ar}.$$

The Super-Kamiokande detector also made measurements of the solar neutrino flux with E_ν greater than about 6 Mev (Fukuda *et al.* 1996).

Because of the high energy threshold these measurements were blind to the principal flux from the 'pp' reaction. The GALLEX (Italy) and SAGE (Russia)

https://doi.org/10.1017/9781009401685.022 Published online by Cambridge University Press

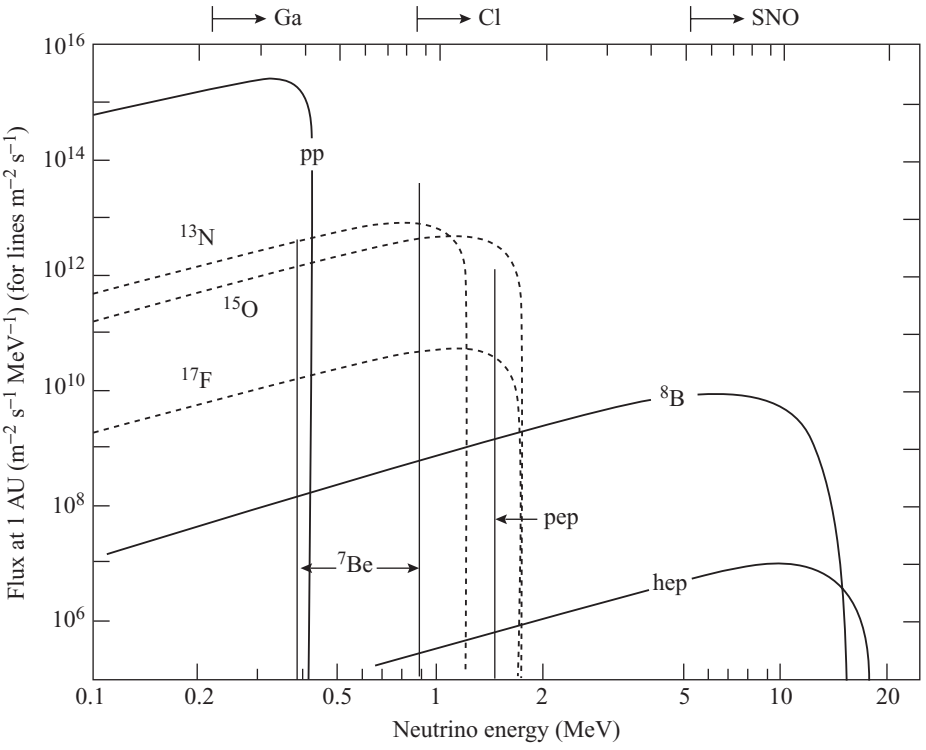

Figure 20.5 The solar neutrino spectra predicted by the standard solar model. Spectra for the pp chain are shown by solid lines and those for the CNO chain by dashed lines. (See Bahcall, J. N. and Ulrich, R. K. (1988), *Rev. Mod. Phys.* **60**, 297.)

experiments were designed to remedy this, and examine the pp flux through the reaction (Hampel *et al.*, 1999; Gavrin *et al.*, 2003)

$$\nu_e + {}^{17}_{31}\mathrm{Ga} + 0.23\ \mathrm{MeV} \rightarrow {}^{71}_{32}\mathrm{Ge} + e^-.$$

The SNO (Sudbury Neutrino Observatory, Canada) is a heavy water detector. Neutrinos, with E_ν greater than about 5 Mev, are detected through the reactions, (Ahmad *et al.* 2002)

$$\nu_e + D_2 + 1.44\ \mathrm{MeV} \rightarrow e^- + p + p,$$
$$\nu_e + D_2 + 2.22\ \mathrm{MeV} \rightarrow p + n + \nu.$$

The first of these reactions is a charged current interaction and can be initiated only by an electron neutrino. The second is a neutral current interaction, initiated with

https://doi.org/10.1017/9781009401685.022 Published online by Cambridge University Press

equal probability by an electron, muon or tau neutrino. The SNO experiment also measured the reaction rate of elastic neutrino scattering from electrons,

$$\nu + e^- \rightarrow \nu + e^-.$$

Again, this reaction can be triggered by a neutrino of any type. Measurements can be used to infer both the ν_e flux $\phi(\nu_e)$ and the total flux $\phi(\nu_e + \nu_\mu + \nu_\tau)$.

The early results from the Homestake detector gave a measured flux of only about one third of that expected from the standard Solar Model without oscillation. Super Kamiokande, GALLEX and SAGE gave about half the expected rate. SNO found that

$$\frac{\phi(\nu_e)}{\phi(\nu_e + \nu_\mu + \nu_\tau)} = 0.306 \pm 0.05.$$

The measured total neutrino flux was consistent with that expected from the Standard Solar Model and clearly, since the Sun produces only electron neutrinos, many have made the transition to ν_μ and ν_τ.

20.7 Solar MSW effects

We showed in Section 19.4 that plane wave neutrino mass eigenstates depended on functions $f_i(z)$, that satisfied

$$i\frac{df_i}{dz} = \frac{m_i^2}{2E} f_i + V(z) U_{ej}^* U_{ei} f_j. \tag{20.6}$$

The source of solar neutrinos is the central region of the Sun, where the Standard Solar Model gives $V(o) = 7.6 \times 10^{-12}$ eV. Comparing this with $\Delta m_{21}^2/2E$, which with the 'reference parameters' of Section 20.1 equals $3.5 \times 10^{-12}(10\,\text{MeV}/E_\nu)$, it is clear that the interpretation of the data from solar neutrino experiments requires a serious consideration of the MSW effect.

As a starting approximation we again neglect the small term U_{e3}. With $U_{e3} = 0$ the solution of (20.6) for $f_3(z)$ is

$$f_3(z) = e^{im_3^2 z/2E} f_3(0),$$

independent of $V(z)$. With $U_{e3} = 0$, and since the initial neutrino is an electron neutrino, $f_3(0) = 0$ and it follows that $f_3(z)$ is zero for all z: it plays no part in the oscillations. The approximation again reduces the analysis to a two-neutrino phenomenon in $f_1(z)$ and $f_2(z)$. After some algebra it can be shown that the solar

https://doi.org/10.1017/9781009401685.022 Published online by Cambridge University Press

neutrino data can be analysed with the equations

$$\begin{aligned} \mathrm{i}\frac{\mathrm{d}f_{\mathrm{e}}}{\mathrm{d}z} &= \frac{\Delta m^2_{21}}{2E}(-\cos(2\theta_{\mathrm{e}2})f_{\mathrm{e}} + \sin(2\theta_{\mathrm{e}2})f_x) + V(z)f_{\mathrm{e}} \\ \mathrm{i}\frac{df_x}{dz} &= \frac{\Delta m^2_{21}}{2E}(\sin(2\theta_{e2})f_e + (\cos 2\theta_{e2})f_x). \end{aligned} \tag{20.7}$$

$f_x = c_{\mu 3} f_\mu - s_{\mu 3} f_\tau$ is a combination of f_μ and f_τ, $V(z)$ is known from the Standard Solar Model. The equations have to be integrated numerically.

All the solar neutrino data is consistent with the oscillation interpretation, and analysis of the data gives $3 \times 10^{-5}\,\mathrm{eV}^2 < \Delta m^2_{21} < 1.9 \times 10^{-4}\,\mathrm{eV}^2$, $30.2^\circ < \theta_{\mathrm{e}2} < 34.9^\circ$ with high probability (95% confidence level). The best fit is with $\Delta m^2_{21} = 6.9 \times 10^{-5}\,\mathrm{eV}^2$, $\theta_{\mathrm{e}2} = 32^\circ$.

The solar neutrino data give a tighter constraint on $\theta_{\mathrm{e}2}$ than KamLAND. Also, with the MSW effect, the solution of equations (20.7) depends on the sign of Δm^2_{21}. It is found to be positive, as is indicated in Figure 20.1

20.8 Future prospects

There are several planned experiments that will make a more thorough investigation of neutrino masses and mixing phenomena. Apart from the possibility of sterile neutrinos, indications of which have not been confirmed, there is no evidence to contradict the three-neutrino theory of Chapter 19. However, it can be seen from the quality of the data presented in this chapter that the neutrino mass theory is not as well established as other branches of The Standard Model. Within the theory experiments are planned to make more precise measurements of the Δm^2 and the parameters of the neutrino mixing matrix.

The principal focus of experimental activity is on the construction of muon neutrino beams as in the K2K experiment. An advantage of accelerator-generated neutrinos is the control that one has on the flux and energy distribution. K2K is an ongoing experiment but by late 2006 the muon neutrino experiments CNGS and MINOS (Main Injector Neutrino Oscillation Search) will be in operation. The CNGS neutrinos are generated at CERN and detected at the GRAN SASSO underground laboratory in Italy. The MINOS beam is generated at Fermilab and detected in the Soudan mine in Minnesota. Both experiments will look for evidence of the rare $\nu_\mu \to \nu_{\mathrm{e}}$ transition and for the expected $\nu_\mu \to \nu_\tau$ oscillations. If the theory of Chapter 19 is not challenged it is expected that by 2010 we will have much tighter bounds on both $\sin^2(2\theta_{\mathrm{e}3})$ and $|\Delta m^2_{\mathrm{At}}|$.

In the more distant future a new very high intensity proton accelerator will be built at Tokai, Japan. The experiment T2K will take over from K2K with a neutrino beam of much higher intensity. Detection at Super Kamiokande will give a base line

https://doi.org/10.1017/9781009401685.022 Published online by Cambridge University Press

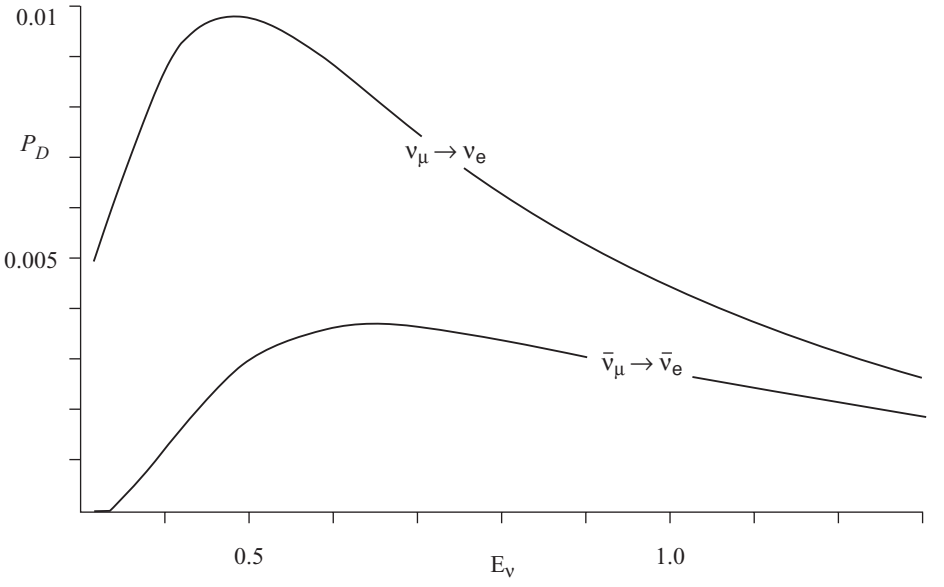

Figure 20.6 The upper curve is $P_D(\nu_\mu \to \nu_e)$.
The lower curve $P_D(\bar{\nu}_\mu \to \bar{\nu}_e)$.
The parameters are $\Delta m^2_{32} = 2 \times 10^{-3}\,\text{eV}^2$, $\Delta m^2_{21} = 7 \times 10^{-5}\,\text{eV}^2$, $\cos\theta_{e2} = 0.84$, $\cos\theta_{\mu 3} = 1/\sqrt{2}$, $\sin\theta_{e3} = 0.05$, $\delta = \pi/4$, $D = 295$ km. The MSW effect, which depends on the local geology will be significant but calculable. It is not included here.

$D \approx 295$ km. An upgrade to higher intensity for MINOS is also planned with a new experiment NOνA. By 2015 with T2K and NOνA it is expected that if $\sin^2(2\theta_{e3}) > 0.01$ then it will be detected. The MSW effect will influence these measurements and the sign of Δm^2_{32} could be established, and hence the mass ordering. If $\sin^2(2\theta_{e3})$ can be measured then it is also possible to have a measurement of the *CP* violating phase δ. Figure 20.6 shows the transition probabilities $P_D(\nu_\mu \to \nu_e)$ and $P_D(\bar{\nu}_\mu \to \bar{\nu}_e)$ as a function of E_ν with the T2K baseline. δ is taken as 45° and the other parameters are a plausible set. Although the probabilities are small, the particle and antiparticle probabilities differ considerably (see Section 19.3).

https://doi.org/10.1017/9781009401685.022 Published online by Cambridge University Press